Chapter 55
Slope Failures and Timing of Turbidity Flows North of Puerto Rico

Jason D. Chaytor and Uri S. ten Brink

Abstract The submerged carbonate platform north of Puerto Rico terminates in a high (3,000–4,000 m) and in places steep (>45°) slope characterized by numerous landslide scarps including two 30–50 km-wide amphitheater-shaped features. The origin of the steep platform edge and the amphitheaters has been attributed to: (1) catastrophic failure, or (2) localized failures and progressive erosion. Determining which of the two mechanisms has shaped the platform edge is critically important in understanding landslide-generated tsunami hazards in the region. Multibeam bathymetry, seismic reflection profiles, and a suite sediment cores from the Puerto Rico Trench and the slope between the trench and the platform edge were used to test these two hypotheses. Deposits within trench axis and at the base of the slope are predominantly composed of sandy carbonate turbidites and pelagic sediment with inter-fingering of chaotic debris units. Regionally-correlated turbidites within the upper 10 m of the trench sediments were dated between ~25 and 22 kyrs and ~18–19 kyrs for the penultimate and most recent events, respectively. Deposits on the slope are laterally discontinuous and vary from thin layers of fragmented carbonate platform material to thick pelagic layers. Large debris blocks or lobes are absent within the near-surface deposits at the trench axis and the base of slope basins. Progressive small-scale scalloping and self-erosion of the carbonate platform and underlying stratigraphy appears to be the most likely mechanism for recent development of the amphitheaters. These smaller scale failures may lead to the generation of tsunamis with local, rather than regional, impact.

Keywords Radiocarbon • Multibeam bathymetry • Mass transport deposits • Seismic reflection

J.D. Chaytor (✉)
U.S. Geological Survey, 384 Woods Hole Road, Woods Hole, MA, USA
e-mail: jchaytor@usgs.gov

U.S. ten Brink
U.S. Geological Survey, Woods Hole Coastal and Marine Science Center,
Woods Hole, MA 02543, USA

S. Krastel et al. (eds.), *Submarine Mass Movements and Their Consequences*, Advances in Natural and Technological Hazards Research 37, DOI 10.1007/978-3-319-00972-8_55,
© Springer International Publishing Switzerland 2014

55.1 Introduction

The style, size, and hazard potential of slope failures along margins of the Puerto Rico Trench (PRT; Fig. 55.1) have been investigated and debated since the first geophysical surveys of the region more than 60 years ago. Thick deposits, primarily composed of turbidite layers in the PRT basins, thought to be the result of turbid flows originating from the Puerto Rico-Virgin Islands (PR-VI) carbonate platform, have received considerable attention through geophysical and sedimentological investigation (e.g., Ewing and Ewing 1962; Conolly and Ewing 1967; Doull 1983). Large-scale indentations (Fig. 55.1), crescentic fracturing, and block detachment along the northern edge of the carbonate platform have all been interpreted to be related to catastrophic failure (Schwab et al. 1991; Hearne 2004) or as a result of localized failures and progressive erosion (Scanlon and Masson 1996; ten Brink et al. 2006).

Determining the ages and mechanisms of major failure events is critically important in the evaluation of regional and Atlantic Ocean-wide geohazards. Catastrophic slope failure would have evacuated more than 1,500 km^3 of material (Schwab et al. 1991), capable of generating a locally destructive, and regionally damaging, tsunami. A smaller slope failure along part of the trench marginal slope (ten Brink et al. 2006), although potentially destructive in the near-field (e.g., the 1918 Mona Canyon tsunami, López-Venegas et al. 2008), would be far less damaging regionally.

Here we report on the analysis of new gravity cores and existing piston cores coupled to a new suite of geophysical data providing insight into mass transport processes (MTPs) in the PRT region. Radiocarbon ages for cores tied to previously identified and correlated turbidites elucidate the recent history of MTPs and landslide-tsunami hazards in the region.

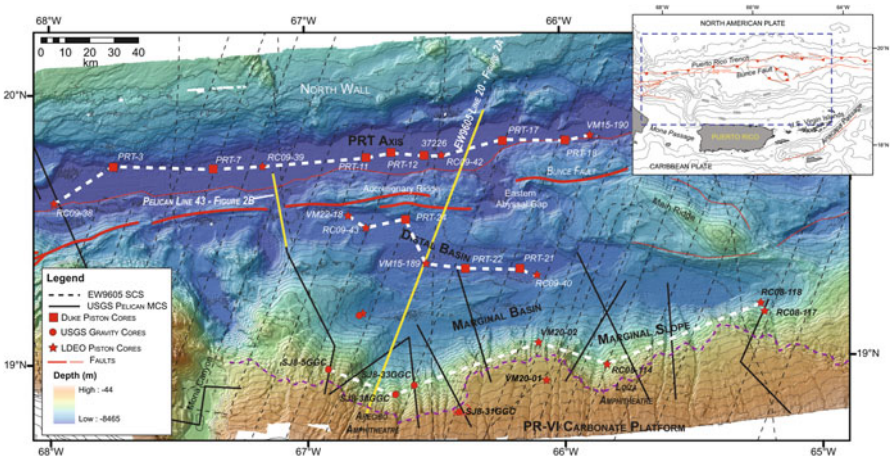

Fig. 55.1 Bathymetry of Puerto Rico Trench and adjacent regions, with primary physiographic features labeled. Core locations, multichannel and single channel seismic line tracks, major faults and the location of core correlation plots (Figs. 55.3, 55.4, and 55.5) are shown

55.1.1 Physiography and Geology

The physiographic subdivisions of the PRT based on the new bathymetry compilation are shown in Fig. 55.1. The Tertiary-age PR-VI carbonate platform, the primary source of material being transported into the PRT, extends from the coastal hills of northern Puerto Rico offshore to a depth of between ~2,500 m (within amphitheaters) and ~4,000 m, with a post-3.3 Ma northward dip of 4°. Deposits of skeletal calcareous sand and river-derived terrestrial material are found on the shelf and upper slope (Schneidermann et al. 1976). Small translational landslides, fractures and dissolution features, and predominantly N-S oriented canyon systems with relief between 100 and 400 m and U- and V-shaped floors (Scanlon and Masson 1996) ornament the carbonate platform. Although the canyon walls are steep (often >20°), covered by varying thicknesses of sediment, and cut by vertical fissures, Gardner et al. (1980) found them to be devoid of evidence of active depositional processes (e.g., turbidity currents, wall failure) and to now be acting as catchments for river-supplied terrestrial material. Based on GLORIA side-scan imagery, Scanlon and Masson (1996) noted that several of these canyons appeared to continue below the marginal escarpment down into the marginal slope, but their full downslope extent and relationship to deposition in the trench could not be determined. ten Brink et al. (2006) mapped 160 landslide evacuation zones along the marginal escarpment and slope, although none exceeded 20 km^3.

55.1.2 Data

Multibeam data, gridded at a resolution of 150 m, covering the bulk of the PRT, were collected by the U.S. Geological Survey (USGS) between 2002 and 2006 using the SeaBeam 2112 system on the National Oceanic and Atmospheric Administration (NOAA) ship *Ronald H. Brown* (Fig. 55.1). Additional bathymetry coverage of the upper carbonate platform (<1,700 m depth) was derived from the NOAA Puerto Rico DEM Discovery Portal (http://www.ngdc.noaa.gov/mgg/dem/demportal.html). Previously collected single-channel (SCS) and new multi-channel (MCS) seismic reflection data were analyzed to identify evidence of slope failure and mass transport processes. Approximately 670 km of MCS reflection profiles crossing the carbonate platform and trench were collected by the USGS in 2006 using a 35 in^3 generated injection gun, and a 24-channel streamer (see Chaytor and ten Brink 2010). SCS profiles used were collected in 1996 aboard the R/V Ewing (cruise EW9605; see van Gestel et al. 1998 for details).

Sedimentology data were derived from eight new gravity cores (SJ8 cores) collected by the USGS in 2008, from cores archived at the Lamont Doherty Earth Observatory (LDEO) core repository (core identifiers RC08/09-xx and VMxx-xx), and from unpublished sources (PRT and 372xx cores, Doull 1983). The USGS cores were collected at sites immediately below the carbonate platform marginal

Table 55.1 AMS ^{14}C radiocarbon ages and 2-σ calibrated age ranges of mixed planktonic foraminifera samples. Radiocarbon ages were converted to calibrated ages using Calib 6.0 (Stuiver and Reimer 1993), utilizing the Marine09 calibration curves (Reimer et al. 2009) and include open ocean 400 year marine reservoir correction

Core	Water depth (m)	Depth in core (cm)	Lab code	Radiocarbon age	2-σ Calibrated age range (BP)
RC08-118	6,190	17–21	OS-76016	6,960 ± 55	7,458 ± 105
RC09-38	8,292	400–403	OS-77358	19,300 ± 85	22,731 ± 504
RC09-39	8,316	694–697	OS-77360	19,350 ± 80	22,713 ± 531
RC09-40	7,817	368–370	OS-77359	16,650 ± 75	19,257 ± 323
		370–372	OS-77361	15,400 ± 60	18,268 ± 272
RC09-42	8,292	230–233	OS-77362	21,700 ± 90	25,449 ± 398
RC09-43	7,815	265–268	OS-76017	16,050 ± 65	18,787 ± 161
		334–338	OS-77363	14,250 ± 55[a]	16,943 ± 182
VM20-02	2,989	16–20	OS-76018	13,050 ± 80	14,848 ± 605
VM22-18	7,948	26–29	OS-76019	11,250 ± 50	12,742 ± 142
SJ8-33GGC	4,912	49–50.5	OS-86482	29,000 ± 120	32,948 ± 503
		90–92	OS-86483	29,300 ± 140	33,706 ± 737
SJ8-38GGC	4564	144–146	OS-86484	44,400 ± 550	47,262 ± 1,442

[a]Age from very small sample, not used in analysis

escarpment. These new cores were visually logged and underwent grain-size, wet bulk density, magnetic susceptibility, and X-ray fluorescence analyses.

Mixed planktonic foraminiferal assemblages (primarily *Globigerinoides ruber* [white], *Globigerinoides sacculifer*, and *Globigerinella aequilateralis*) extracted from the newly collected gravity cores and LDEO piston cores were radiocarbon dated at the National Ocean Sciences Accelerator Mass Spectrometry facility (Table 55.1). Although much of the PRT and adjacent area lies below the regional carbonate compensation depth, carbonate preservation in the samples was high, possibly due to rapid burial by turbidity currents and debris flows. Given the age (greater than 50 years) and sampling history of the LDEO cores, the sampled intervals often consisted of several centimeters of sediment below event layers and therefore their ages likely have lower precision.

55.2 Results

55.2.1 Slope Failure Features and Mass Transport Deposit Distribution

Mass Transport Deposits (MTD) associated with failures of the slope north of Puerto Rico appear to be confined to surficial slope deposits, base of slope debris wedges and turbidites, and thin debris flow layers in the marginal and distal

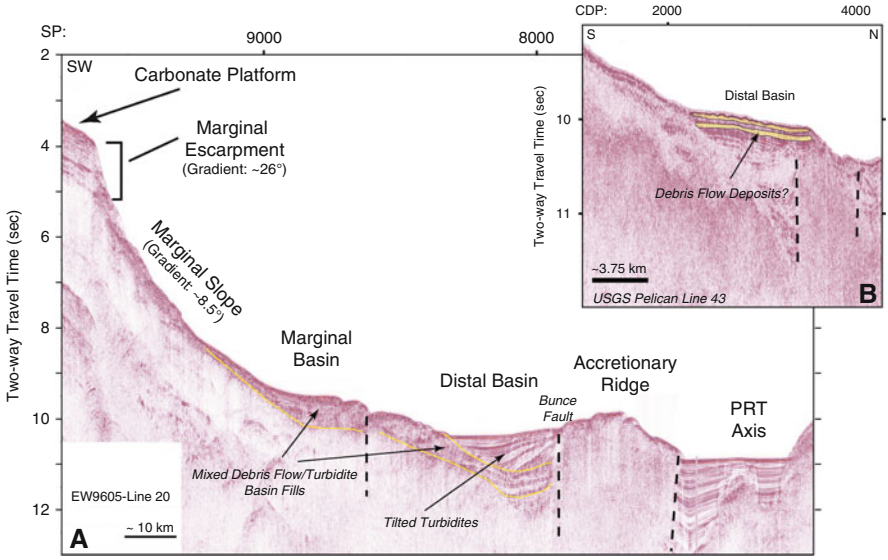

Fig. 55.2 (**a**) Stacked single-channel seismic line EW9605-Line 20 showing the general physiographic components of the trench and its margins (outlined by *yellow line*). Turbidite and debris flow deposition are seen on the marginal slope and in the marginal basin, while generally only turbidites are seen in the distal basin and PRT axis. *Dashed lines* mark the location of faults. (**b**) USGS MCS Line 43 showing the presence of a near-surface debris flow deposit at the western end of the distal basin (location in *yellow* on Fig. 55.1)

basins and the trench axis (Fig. 55.2a). While debris flow deposits appear to be generally confined to the marginal slope and basin, at least one debris flow, from an unknown source, is present in the near surface at the western end of the distal basin (Fig. 55.2b). Most notably, there is no evidence of blocky debris flows or rock falls that would be characteristic of catastrophic failure of amphitheater-scale sections of the competent carbonate platform material and older underlying units. Large-scale blocky submarine slope failures of coherent lithologies have been found to leave a prominent surficial and subsurface record for 10's of thousands to millions of years (e.g., Clague and Moore 2002; Le Friant et al. 2004). Using the new MCS data we have not been able to confirm the presence of detached and down-thrown blocks of carbonate platform material along the marginal slope as reported by Hearne (2004).

As noted by Scanlon and Masson (1996) and revealed in great detail by the new bathymetry data, many of the canyon systems developed in the carbonate platform continue across the marginal escarpment and down the marginal slope (Fig. 55.1). Below the marginal escarpment, the widths of the canyons increase substantially and develop flat to U-shaped floors. The canyon systems do not extend beyond the base of the slope and there is no surficial expression of depositional fans within the marginal or distal basins. The morphology of these canyon systems suggests that they are currently zones of accumulation and have been for some time.

55.2.2 *Correlation and Timing of Turbidite and Debris Flow Deposition*

Correlations of individual turbidite and pelagic units within the PRT basins based on detailed sedimentological analysis have been carried out by Conolly and Ewing (1967) and Doull (1983) and those correlations will generally be applied here. Sediments recovered in the LDEO, Duke and USGS cores along the marginal slope and within the trench basins are classified as (1) pelagic sediments including foraminifera oozes, (2) turbidites and debris flows consisting of calcareous sands often containing carbonate rock fragments, terrigenous material, foraminifera tests and pteropod shells, and often, shallow water organisms, or (3) sediment characterized by silty-clay size fraction composed of a mix of pelagic sediments and silt-sized carbonate and terrigenous rock fragments, usually present above turbidite sands. Sediments on the deeper parts of the carbonate platform are predominantly pelagic in origin, interrupted by only very thin sands containing shallow water material, the youngest of which in core VM20-01 was deposited after approximately 13,000 year BP. Core SJ8-31GGC from within a landslide scar at the edge of the marginal escarpment (Fig. 55.1) contains at least 12 cm of Holocene pelagic sediments (based on the presence of *Globorotalia menardii*).

55.2.2.1 Marginal Slope and Basin

A plot of cores from the marginal slope (Fig. 55.3) reveals strong along-slope variations in near surface sediments. Thick gravel layers in core VM20-01 and clay-breccia interval in core RC08-118 stand as evidence of deposition of small scale MTDs on the slope. Sand layers are almost always ungraded and some contain gravel-size clasts of carbonate rock at their base. All but one of the cores is capped by a layer of pelagic sediment, which in core RC08-118 has a basal age of $7{,}458 \pm 105$ year BP. Core RC08-114 is composed entirely of pelagic sediment layers, suggesting that if the record is complete, there has either been no significant downslope sediment transport or the marginal slope acts more as a "by-pass" slope (Schlager and Camber 1986). Dates of pelagic and silty-clay layers directly above thin sand layers in cores SJ8-33GGC and -38GGC collected on ridges between canyons within the Arecibo Amphitheatre, returned late-Pleistocene ages of $32{,}948 \pm 503$ and $47{,}262 \pm 1{,}442$ years BP, respectively.

55.2.2.2 Distal Basin

Doull (1983) identified four correlatable turbidites in the sediments of the distal basin (EP-1-EP-4), the thickest of which was EP-3 (Fig. 55.4). That said, many of the turbidite sands in the distal basin cores have particularly thick silty-clay tails and multiple sand pulses which complicate correlation along the full length of the

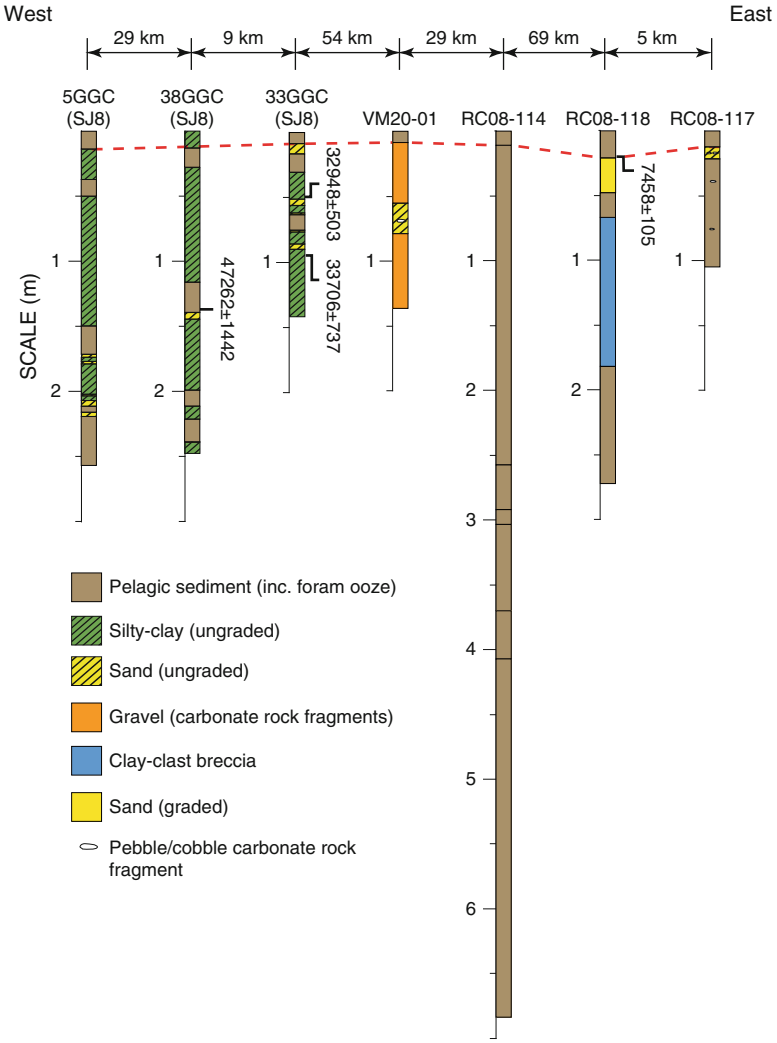

Fig. 55.3 Marginal slope core correlation plot revealing a dynamic and complex depositional environment which varies over relatively short distances. The *red-dashed line* marks the base of the capping pelagic layer. Calibrated AMS ^{14}C radiocarbon ages determined from mixed planktonic foraminifera samples are shown for selected cores (in years BP with 2-σ errors). Location of cores and correlation line shown on Fig. 55.1

basin. A prominent turbidite between the EP-3 and EP-4 turbidites in core RC09-40 interpreted by Doull (1983) to be a surge or pulse of the EP-3 event has an age of between 18,000 and 19,500 year BP (bioturbation may have caused mixing in the sediment prior to turbidity current arrival). A similar age of 18,787 years BP was determined for pelagic sediment at the base of the penultimate turbidite in

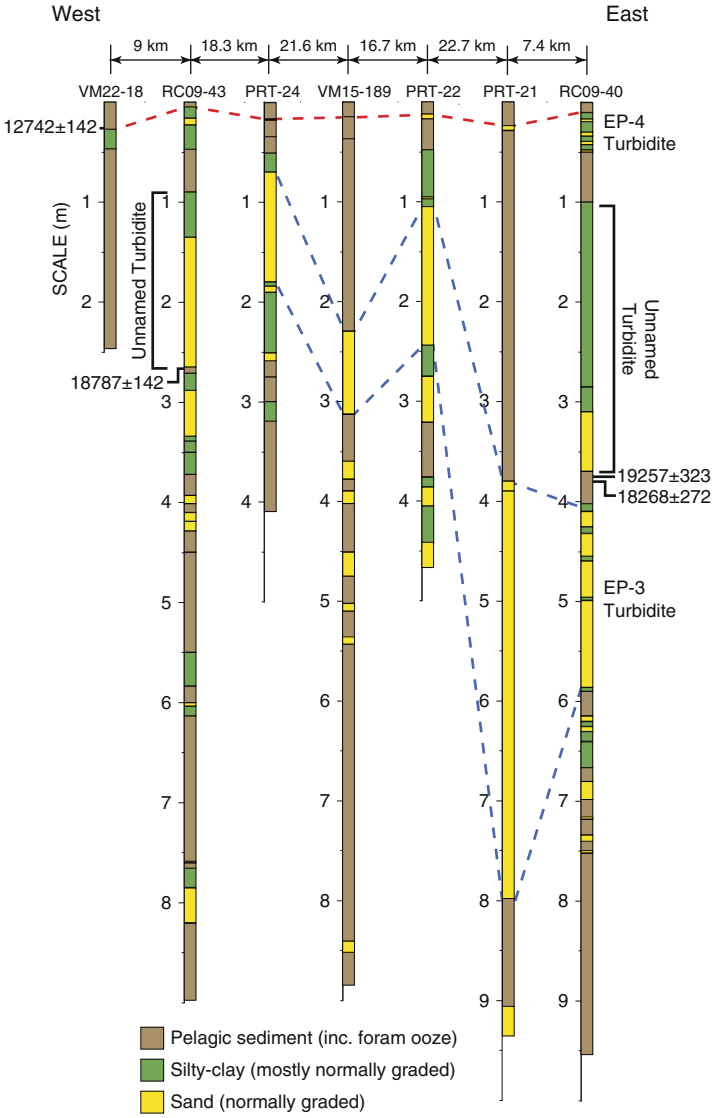

Fig. 55.4 Distal basin core correlation plot. Thick turbidites [Doull (1983) only assumes that the graded sands comprise the turbidite, but they often have a significant graded silty-clay tail] are present throughout the distal basin, the most prominent of which is the EP-3 turbidite. The youngest significant turbidite in RC09-40 (between the EP-4 and EP-3 turbidite of Doull (1983)) and RC09-43 has a basal age of between 18 and 19 ka. *Red dashed line* marks base of capping pelagic layer, *blue lines* mark upper and lower bounds of correlated turbidites. Correlation location shown on Fig. 55.1

RC09-38, which was not included in the Doull (1983) correlation. As with cores of the marginal slope, all cores analyzed in the distal basin are capped with a pelagic layer of variable, but not more than ~ 25 cm thickness. The age at the base of the capping pelagic layer in core VM22-8 at the western end of the distal basin (Fig. 55.4) is 12,742 ± 142 year BP (accumulation rate of ~ 2 cm/1,000 year).

55.2.2.3 PRT Axis

Sediments in the upper 9–10 m of the PRT axis are comprised primarily of pelagic sediments interrupted at various depths by sandy turbidites (Fig. 55.5). Doull (1983) identified three potentially correlative turbidites, although only turbidite MP-2 could be correlated well across the length of the PRT axis and based on turbidite thickness variations, entry point locations, and sand composition, attributed the Puerto Rico slope as the primary source of the material. The estimated volume of the combined MP-2 and EP-3 turbidites is approximately 1.9 km^3 (Doull 1983). As with sediments elsewhere throughout the trench, all cores have pelagic sediments of varying thickness at their top. Radiocarbon ages of pelagic sediment immediately below the MP-2 turbidites in cores RC09-38, RC09-39, and RC09-42 were found to be 22,731, 22,713, and 25,449 year BP, respectively. The 3,000 year older age in core RC09-42 may reflect additional erosion of pelagic material by the turbidity current, especially if this core was more proximal to the turbidity current entry point (eastern abyssal gap, Fig. 55.1) into the PRT axis.

55.3 Discussion and Conclusions

Geologic and geophysical data from the PRT show that mass transport processes, while prevalent across the entire region, may be spatially and temporally restricted. While attempts have been made to assign specific source areas along the edge of the carbonate platform to imaged deposits (Hearne 2004), such determinations are difficult and prone to error given the complex mixing of slope failure and channel flushing material from multiple sources and the ongoing tectonic deformation within the PRT.

Our analysis of available bathymetry, seismic reflection, and core data indicates that there has not been any large-scale collapse of the carbonate platform and/or marginal slope during the Late Pleistocene-Holocene. A lack of wide-spread deposition of blocky carbonate platform fragments in debris flow material strongly supports a process of progressive erosion and dissolution (scalloping, Mullins and Hine (1989); self-erosion, Schlager and Camber (1986)) and infrequent slope channel flushing as the primary sources of mass transport material entering the PRT basins. In fact the turbidites/debris flows penetrated by the cores are likely the result

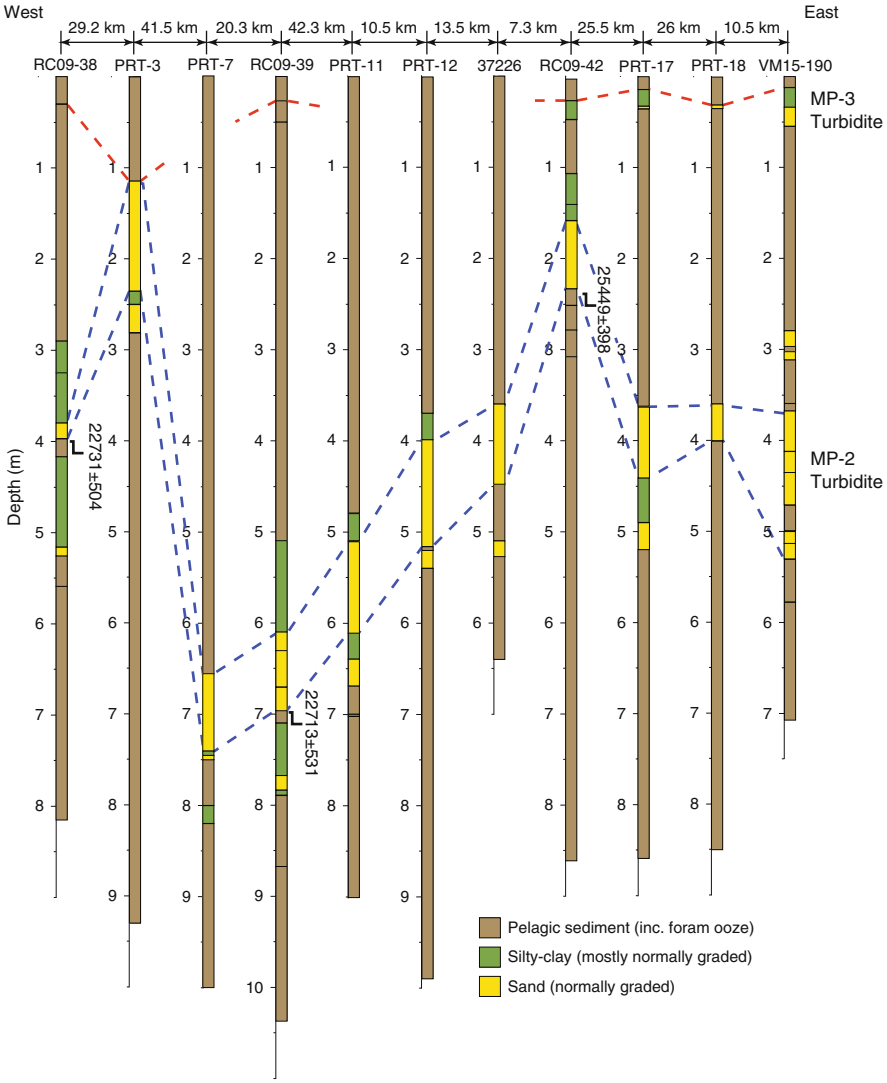

Fig. 55.5 PRT axis core correlation plot. Thick turbidites are less common than in the distal basin. The capping pelagic layer (base marked by *dashed red line*) is discontinuous across the PRT axis. Age of the MP-2 turbidite (*blue dashed lines*) is between 22.7 and 25.5 ka

of minor destabilization/channel flushing events given that Doull (1983) calculated the combined volume of the MP-2 and EP-3 turbidites to be only 1.9 km^3, ten times smaller than the maximum evacuation scar mapped by ten Brink et al. (2006) along the marginal slope. Interestingly, although the trench is a seismically active plate boundary, we find that there has not been significant turbidity current or debris flow activity within the trench for the last 18,000 years.

From a landslide-tsunami hazards perspective, long-term progressive margin erosion resulting in many small-scale failures suggests that there is currently a low probability of occurrence of a regionally destructive landslide-generated tsunami from the slope north of Puerto Rico. Non-catastrophic failure during the late Pleistocene-Holocene period may also indicate that the PRT has not experienced a high magnitude (>M8) earthquake capable of destabilizing large sections of the carbonate platform or marginal slope. That said, a landslide and local tsunami hazard does exist due to continued earthquake-triggered scalloping and/or self-erosion of the carbonate platform north of Puerto Rico as shown by the 1918 M7.2 Mona Passage earthquake/landslide and the resulting tsunami (López-Venegas et al. 2008).

Acknowledgments We would like to thank the captain and crew of the R/V Seward Johnson, Jim Broda, Heather Benway, Kate McMullen, and Rusty Lotti Bond and the staff of the LDEO core repository. EW9605 seismic data was acquired from the UTIG Academic Seismic Portal. Kathryn Scanlon, Lorena Moscadelli and Calvin Campbell provided valuable reviews. Any use of trade, product, or firm names is for descriptive purposes only and does not imply endorsement by the U.S. Government.

References

Chaytor JD, ten Brink US (2010) Extension in Mona Passage, Northeast Caribbean. Tectonophysics 493:74–92

Clague DA, Moore JG (2002) The proximal part of the giant submarine Wailau landslide, Molokai, Hawaii. J Volcanol Geotherm Res 113:259–287

Conolly J, Ewing M (1967) Sedimentation in the Puerto Rico Trench. J Sediment Res 37:44

Doull ME (1983) Turbidite sedimentation in the Puerto Rico Trench abyssal plain. Masters thesis, Duke University, 248 pp

Ewing J, Ewing M (1962) Reflection profiling in and around the Puerto Rico Trench. J Geophys Res 67:4729–4739

Gardner WD, Glover L, Hollister CD (1980) Canyons off northwest Puerto Rico: studies of their origin and maintenance with the nuclear research submarine NR-1. Mar Geol 37:41–70

Hearne ME (2004) Investigation of submarine landslide deposits the northern margin of Puerto Rico. MS thesis, University of North Carolina Wilmington, 84 pp

Le Friant A, Harford CL, Deplus C et al (2004) Geomorphological evolution of Montserrat (West Indies): importance of flank collapse and erosional processes. J Geol Soc Lond 161:147–160

López-Venegas A, ten Brink US, Geist EL (2008) Submarine landslide as the source for the October 11, 1918 Mona Passage tsunami: observations and modeling. Mar Geol 254:35–46

Mullins HT, Hine AC (1989) Scalloped bank margins: beginning of the end for carbonate platforms? Geology 17:30–33

Reimer P, Baillie M, Bard E et al (2009) INTCAL09 and MARINE09 radiocarbon age calibration curves, 0–50,000 years cal BP. Radiocarbon 51:1111–1150

Scanlon KM, Masson DG (1996) Sedimentary processes in a tectonically active region: Puerto Rico North Insular Slope. In: Gardner JV, Field ME, Twichell DC (eds) Geology of the US seafloor: the view from GLORIA. Cambridge University Press, Cambridge, pp 123–134

Schlager W, Camber O (1986) Submarine slope angles, drowning unconformities, and self-erosion of limestone escarpments. Geology 14:762–765

Schneidermann N, Pilkey OH, Saunders C (1976) Sedimentation on the Puerto Rico insular shelf. J Sediment Res 46:167–173

Schwab W, Danforth W, Scanlon K et al (1991) A giant submarine slope failure on the northern insular slope of Puerto Rico. Mar Geol 96:237–246

Stuiver M, Reimer PJ (1993) Extended 14C database and revised CALIB radiocarbon calibration program. Radiocarbon 35:215–230

ten Brink US, Geist EL, Andrews BD (2006) Size distribution of submarine landslides and its implication to tsunami hazard in Puerto Rico. Geophys Res Lett 33:L11307. doi:10.1029/2006GL26125

van Gestel JP, Mann P, Dolan JF et al (1998) Structure and tectonics of the upper Cenozoic Puerto Rico-Virgin Islands carbonate platform as determined from seismic reflection studies. J Geophys Res 103:30505–30530